The Journal of Experimental Biology 212, 3283-3295
Published by The Company of Biologists 2009
doi:10.1242/jeb.033910

The involvement of SLC26 anion transporters in chloride uptake in zebrafish (*Danio rerio*) larvae

M. Bayaa[1], B. Vulesevic[1], A. Esbaugh[1], M. Braun[1], M. E. Ekker[1], M. Grosell[2] and S. F. Perry[1,*]

[1]Department of Biology and Centre for Advanced Research in Environmental Genomics, University of Ottawa, Ottawa, Ontario K1N 6N5, Canada and [2]Rosenstiel School of Marine and Atmospheric Science, University of Miami, Miami, FL 33149, USA

*Author for correspondence (sfperry@uottawa.ca)

Accepted 8 July 2009

SUMMARY

After demonstrating phylogenetic relatedness to orthologous mammalian genes, tools were developed to investigate the roles of three members (A3, A4 and A6c) of the SLC26 anion exchange gene family in Cl^- uptake and HCO_3 excretion in embryos and larvae of zebrafish (*Danio rerio*). Whole-mount *in situ* hybridization revealed the presence of SLC26 mRNA in gill primordia, mesonephros and heart (*slc26a3* and *a4* only) at 5–9 days postfertilization (d.p.f.). SLC26A3 protein was highly expressed in lateral line neuromasts and within the gill, was localized to a sub-population of epithelial cells, which often (but not always) coexpressed Na^+/K^+-ATPase. SLC26 mRNA levels increased with developmental age, peaking at 5–10 d.p.f.; the largest increases in rates of Cl^- uptake ($J_{in}^{Cl^-}$) preceded the mRNA spike, occurring at 2–5 d.p.f. Raising zebrafish in water with a low [Cl^-] caused marked increases in $J_{in}^{Cl^-}$ at 3–10 d.p.f. and was associated with increased levels of SLC26 mRNA. Raising fish in water of high [Cl^-] was without effect on $J_{in}^{Cl^-}$ or SLC26 transcript abundance. Selective gene knockdown using morpholino antisense oligonucleotides demonstrated a significant role for SLC26A3 in Cl^- uptake in larval fish raised in control water and roles for A3, A4 and A6c in fish raised in water with low [Cl^-]. Prolonged (7 days) or acute (24 h) exposure of fish to elevated (2 or 5 mmol l^{-1}) ambient [HCO_3^-] caused marked increases in Cl^- uptake when determined in water of normal [HCO_3^-] that were accompanied by elevated levels of SLC26 mRNA. The increases in $J_{in}^{Cl^-}$ associated with high ambient [HCO_3^-] were not observed in the *SLC26* morphants (significant only at 5 mmol l^{-1} HCO_3^- for *A4* and 2 mmol l^{-1} HCO_3^- for *A6c*). Net base excretion was markedly inhibited in the *slc26a3* and *a6c* morphants thereby implicating these genes in Cl^-/HCO_3^- exchange. The results suggest that under normal conditions, Cl^- uptake in zebrafish larvae is mediated by SLC26A3 Cl^-/HCO_3^- exchangers but under conditions necessitating higher rates of high affinity Cl^- uptake, SlC26A4 and SLC26A6c may assume a greater role.

Key words: SLC26A3, SLC26A4, SLC26A6, pendrin, ionic regulation, acid–base balance, mitochondrion rich cell, gill, DRA, PAT1.

INTRODUCTION

Fishes inhabiting freshwater (FW) continually lose Cl^- and other ions by diffusion across the gill to the surrounding water and to a much lesser extent by urinary excretion. Although there are some notable exceptions of fish lacking appreciable Cl^- uptake capacity [*Lepomis macrochirus* (Tomasso and Grosell, 2005), *Anguilla rostrata* or *A. anguilla* (Goss and Perry, 1994) and *Fundulus heteroclitus* (Patrick et al., 1997)], in most FW fish species that have been examined, internal Cl^- balance is maintained in the face of these diffusive losses by constant replenishment *via* the active absorption of Cl^- at the gill. More than 70 years ago it was suggested that Cl^- uptake across the gill occurs by Cl^-/HCO_3^- exchange (Krogh, 1937) yet the specific identity of the exchange protein(s) still remains unknown. Although evidence is sparse, members of two gene families have been implicated in branchial Cl^-/HCO_3^- exchange; the SLC4 bicarbonate transporters (for reviews, see Alper et al., 2002; Romero et al., 2004; Alper, 2006; Pushkin and Kurtz, 2006) and the SLC26 anion transporters (for reviews, see Mount and Romero, 2004; Romero et al., 2006; Soleimani and Xu, 2006; Sindic et al., 2007; Ohana et al., 2009). Members of the SLC4 family specifically translocate HCO_3^- or CO_3^{2-} (Pushkin and Kurtz, 2006) either in a sodium-independent (AE1–4) or sodium-dependent manner.

The SLC26 proteins can be distinguished from the SLC4 transporters because they are largely sodium-independent and promiscuously transfer a variety of anions including Cl^-, HCO_3^-, OH^-, SO_4^{2-}, formate, oxalate and iodide. Immunohistochemical evidence for the involvement of SLC4A1 (AE1) in branchial Cl^-/HCO_3^- exchange was provided by Wilson (Wilson et al., 2000) who reported the presence of AE1-like protein on the gills of tilapia (*Oreochromis mossambicus*) using a heterologous antibody. Similarly, evidence for a role of SLC26A4 was obtained by its immunolocalization in gills of FW Atlantic stingray, *Dasyatis sabina* (Piermarini et al., 2002).

In recent years, the zebrafish (*Danio rerio*) has emerged as a powerful model for studying piscine ionic regulation owing to the nearly complete annotation of its genome and the ability to perform gene silencing experiments on larvae (Pan et al., 2005; Lin et al., 2005; Yan et al., 2007). Adult zebrafish have an extremely high affinity and high capacity Cl^- uptake mechanism which is appropriately regulated depending on environmental constraints (Boisen et al., 2003). Thus, zebrafish would seem to offer significant advantages over other species in ongoing attempts to delineate the molecular mechanisms of branchial Cl^-/HCO_3^- exchange. In the present study we have focused on three members of the SLC26 gene family as possible candidates for Cl^- uptake in zebrafish; SLC26A3 (also known as down-regulated in adenoma; DRA), SLC26A4 (pendrin) and SLC26A6 (also known as proton-coupled amino acid transporter 1; PAT1). These three members were selected because they all are known to exhibit Cl^-/HCO_3^- exchange activity (Mount

and Romero, 2004). Using this approach, we were able to develop morpholino antisense oligonucleotides to knockdown (Nasevicius and Ekker, 2000) these three SLC26 genes during development and thereby evaluate their roles in Cl^- uptake and base excretion.

MATERIALS AND METHODS

Experimental animals and holding conditions

Ottawa

Adult zebrafish (*Danio rerio* Hamilton; 400–800 mg) were obtained commercially from Big Al's Aquarium Services (Ottawa, Canada). The fish were kept in plastic aquaria supplied with recirculating, filtered and dechlorinated fresh water. Fish were maintained at 28°C on a 14 h:10 h light:dark photoperiod and were fed daily using a commercial fish diet (Westerfield, 2007). Groups of five to eight fish were acclimatized to differing environmental conditions for 7 days prior to experimentation. The different conditions were as follows: dechlorinated fresh water (hereafter referred to as control), low and high chloride water, with final chloride concentrations of 0.02 and 2.0 mmol l^{-1}, respectively, and base water (control water supplemented with either 2 or 5 mmol l^{-1} $NaHCO_3$). The ionic composition of control water was 0.8 mmol l^{-1} Na^+, 0.4 mmol l^{-1} Cl^-, 0.25 mmol l^{-1} Ca^{2+}, 0.03 mmol l^{-1} K^+. Low and high Cl^- media were prepared by combining appropriate quantities of NaCl and with other salts as required ($CaSO_4 \cdot 2H_2O$, $NaSO_4$, K_2HPO_4) in reverse osmosis water.

Embryos were obtained using standard techniques for zebrafish breeding (Westerfield, 2007) and newly spawned eggs were collected from random groups of adult breeders and kept in rearing tanks at 28°C until needed. All procedures involving animal use were carried out according to institutional guidelines and in accordance with those of the Canadian Council on Animal Care (CCAC).

Miami

Measurements of net acid excretion were performed in Miami. Fish used for breeding were obtained from Aquatica tropical, Miami, FL, USA and were maintained in dechlorinated city of Miami tap water [for water composition see Bielmyer et al. (Bielmyer et al., 2007)]. Fertilized eggs were obtained according to standard protocols for zebrafish breeding (Westerfield, 2007). All procedures on zebrafish were in accordance with University of Miami's Institutional Animal Care and Use Committee.

Sequence and phylogenetic analysis

Putative zebrafish orthologs of SLC26A3, A4 and A6c were obtained by using BLAST analysis of nucleotide or amino acid sequences of human SLC26 genes (GenBank Accession numbers NM_000111, NM_000441 and AB102713) against the Ensembl zebrafish genome (www.ensembl.org). Putative full length orthologs for zA3 (si:dkey-31f5.2), zA4 (si:dkey-31f5.9) and zA6c (zgc:175226) genes were located on chromosomes 4, 4 and 6, respectively. The two putative orthologs for A3 and A4 were fully annotated whereas the presumptive A6c ortholog was assigned a designation of secondary active sulfate transmembrane transporter. It should be noted that at the time of the initial data mining (2003–2004), only a single zA6 gene was identified; only recently was zA6c determined to be one of several zA3 isoforms (see Fig. 1).

A series of phylogenetic analyses of the vertebrate solute carrier 26 (SLC26) proteins was performed. The SLC26 sequences used in the analyses are as follows: *Homo sapiens* A1 (NP_998778), A2 (NP_000103), A3 (NP_000102), A4 (NP_000432), A5 (AAI00834), A6a (NP_075062), A6b (NP_599025), A6c (NP_602298), A6d (NP_001035544), A7 (AAH94730), A7b (NP_599028), A8a (NP_443193), A8b (NP_619732), A9a (NP_443166), A9b (NP_599152), A11 (Q86WA9); *Mus musculus* A1 (AAH32151), A2 (NP_031911), A3 (AAI39274), A4 (NP_035997), A5 (AAI08988), A6 (NP_599252), A7 (NP_666059), A8 (NP_666188), A9 (NP_796217), A11 (NP_848858); *Xenopus laevis* A1 (AAP45002), A3 (AAP37475), A4 (AAQ11740), A6 (AAN85411); *Xenopus tropicalis* A4 (AAI57509), A6 (AAI61524), A6b (NP_001072916), A9 (AAI35994); *Gallus gallus* A5 (NP_001072945); *Takifugu obscurus* A3 (BAE75794), A5 (BAE75795), A6a (BAE75796), A6b (BAE75797), A6c (BAE75798), A11 (BAE75799); *Oncorhynchus mykiss* A1 (NP_001117958); *Opsanus beta* A6 (ABQ01444), A6b (ACF75333); *Anguilla japonica* A1 (BAD22606), A6 (BAC16761), A6b (BAD22607); *Tetraodon nigroviridis* A1 (CAG04906), A2 (CAF95371); *Danio rerio* A1 (NM_001080667), A2 (XP_685114), A3 (FJ170816), A4 (FJ170817), A5a (AAP32789), A5b (NP_958881), A6 (XP_687043), A6 (XP_685992), A6b (XP_001344243), A6c (FJ170818), A11 (NP_956061), unknown (XP_001921766). Amino acid sequence alignments were used for phylogenetic analyses, and were performed using ClustalX (version 1.8). Phylogenetic hypotheses were constructed using both neighbor joining (NJ) and maximum parsimony (MP) techniques using the PAUP* [beta test version 4.0b10] software package. MP analysis consisted of a heuristic search with TBR branch swapping, ACCTRAN character state optimization enforced, with random stepwise additions and 1000 random addition replicates. NJ was performed on a matrix of mean character distances. Support for nodes in both cases was obtained through bootstrap analyses with 1000 pseudoreplicates. In both analyses, gaps were included and treated as missing data, and the urochordate *Ciona intestinalis* SLC26A5 (AAP57206) sequence was used as a an outgroup.

The SLC26 sequences obtained from GenBank were used to design PCR primers for real-time reverse transcriptase PCR and to generate probes for in situ hybridization; these various primers are summarized in Table 1. Additionally, for each gene, primers were designed to amplify PCR products with expected sizes of 1577 (*a3*), 1857 (*a4*) and 1807 (*a6c*) base pairs (Table 1). Analysis of the genomic sequence of si:dkey-31f5.9 (putative SLC26A4) revealed a possible alternative start codon 301 nucleotides upstream of the predicted start codon. Using this region to blast the zebrafish EST database it was confirmed that this region is expressed and indeed contains several highly conserved amino acids. Thus, the forward primer for *a4* was designed from the genomic sequence to potentially amplify a longer cDNA. This resulted in a final cDNA sequence for A4 which was 39 nucleotides longer than si:dkey-31f5.9. Following 3′- and 5′-RACE, sequencing of multiple overlapping clones and contig assembly, final sequences were assembled for SLC26A3 (accession no. FJ170816), SLC16 A4 (accession no. FJ170817) and SLC26A6c (accession no. FJ170818) that were 99–100% identical to the 'in silico' sequences when compared over comparable regions.

RNA extraction, RT-PCR and molecular cloning

Embryonic (<2 d.p.f.), larval (3–30 d.p.f.) and adult zebrafish were killed by anesthetic overdose (0.05 mg ml^{-1} MS-222; ethyl 3-aminobenzoate methanesulfonate; Sigma, St Louis, MO, USA) in control water. Pooled embryos or larvae were rapidly frozen in liquid nitrogen and stored at –80°C. For adults, complete fish were frozen in liquid nitrogen, ground on dry ice using a mortar and pestle and stored at –80°C until the preparation of total RNA.

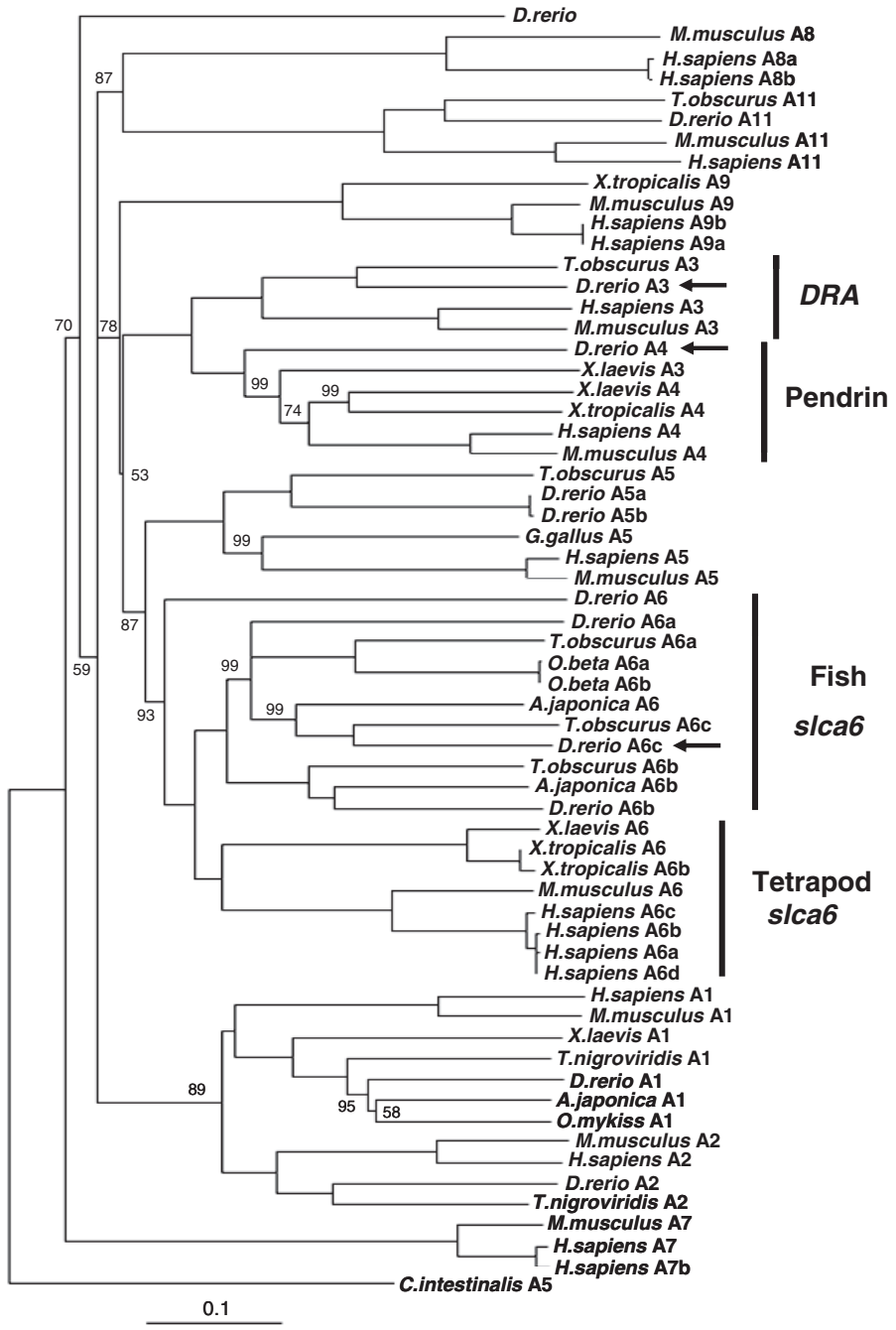

Fig. 1. Phylogenetic analysis of the solute carrier 26 (SLC26) gene family, based on neighbor joining phylogenetic hypotheses. Bootstrap values for nodes are denoted, and branches with less than 50% support were collapsed. Bootstrap values of 100 were not shown on the tree. Branch lengths are drawn to scale with the length of 0.1 approximating replacement of 10% of the amino acids in the protein alignment. The arrows denote the specific *slc26* isoforms that were targeted for knockdown and real time PCR analysis.

Whole body total RNA was isolated from zebrafish using TRIzol reagent (Invitrogen, Burlington, Ontario, Canada) according to the instructions of the manufacturer and 5 μg were reverse transcribed using oligo(dT) primers (Sigma Genosys, Oakville, Ontario, Canada) and Superscript II reverse transcriptase (Invitrogen). PCR products were amplified using the following cycling parameters: 2 min at 94°C followed by 30 cycles of 30 s at 92°C, 30 s at 58°C and 1 min 30 s at 72°C. The final extension of the amplified products was at 72°C for 10 min. The final constitution of the PCR mix was: 1× PCR buffer, 1.5 mmol l^{-1} $MgCl_2$, 0.2 mmol l^{-1} dNTP, 2 pmol each of forward and reverse primers, 2.5 i.u. of Taq polymerase (Invitrogen), and 100 ng of zebrafish gill cDNA. The PCR products were run on a 1.25% agarose gel and purified using a PCR purification kit (Sigma). A PCR cloning kit was used to clone the purified PCR products into a pCR II vector (Invitrogen). The desired clone was purified using a GelElute plasmid miniprep kit (Sigma). Purified plasmids were sequenced using M13 Forward (–20) and M13 Reverse primers.

Quantification of mRNA levels using real-time PCR

Total RNA was extracted from aliquots of powdered tissue samples using the Absolutely RNA RT-PCR Miniprep Kit (Stratagene, Mississauga, Ontario, Canada). To remove any remaining genomic DNA, the RNA was treated on-column using RNase-free DNase (5 μl) for 20 min at room temperature. The RNA was eluted in 50 μl of nuclease-free H_2O and its quality was assessed by gel electrophoresis and spectrophotometry (Eppendorf Biophotometer). The cDNA was synthesized from 1 μg of RNA using random

Table 1. Oligonucleotide primers used for RT-PCR, cDNA cloning, real-time RT-PCR and *in situ* probe construction

Primer name	Primer sequence	Uses	Product size (bp)
ZA3-F	5′-GCTTTTCCAATTCTGAGTCTAATG-3′	*za3* cDNA cloning	1577
ZA3-R	5′-TTCAGACCCTTGAGTGCAG-3′		
ZA4-F	5′-TGGCGATACATCTTGTGGAGTACG-3′	*za4* cDNA cloning	1857
ZA4-R	5′-1857TGAGGCCACTGGTACCAAAC-3′		
ZA6-F	5′-GCACATTTACTATCCTCAGTATTATG-3′	*za6c* cDNA cloning	1807
ZA6-R	5′-GTCTTAATGGCCACGGTATC-3′		
QzActin-F	5′-TCCTGGGTATGGAATCTTGCGGT-3′	QPCR control	122
QzActin-R	5′-GTACATGGTGGTACCTCCAGACAGCA-3′		
QzA3-F	5′-GTTGTTCTGTCCTGGCCAAT-3′	QPCR *za3*	128
QzA3-R	5′-GATGTTAGCAAAGAAGATGGGTGA-3′		
QzA4-F	5′-ATGCAGTGCGGGTGTTCA-3′	QPCR *za4*	110
QzA4-R	5′-TGAGGCCACTGGTACCAAAC-3′		
QzA6-F	5′-ATACCTGAGACAGCACGGACAT-3′	QPCR *za6c*	130
QzA6-R	5′-TGGAGTCAATGGTGGTAACATC-3′		
A3-IS-F	5′-GCTTTTCCAATTCTGAGTCTAATG-3′	Probe construct *za3*	748
A3-IS-R	5′-ATGCTCCAAACATGTTGCTC-3′		
A4-IS-F	5′-AGTGCAACTCGCCGATTTAT-3′	Probe construct *za4*	486
A4-IS-R	5′-AAAAAGACAGGGCCTCCATT-3′		
A6-IS-F	5′-GCACATTTACTATCCTCAGTATTATG-3′	Probe construct *za6c*	805
A6-IS-R	5′-AATTGCATAACCCACAATGG-3′		

hexamer primers (Boehringer-Mannheim, Laval, Quebec, Canada) and Stratascript reverse transcriptase (Stratagene). Relative mRNA levels were assessed by real-time PCR on samples of cDNA (0.5 µl) using a Brilliant SYBR Green QPCR Master Mix Kit (Stratagene) and a Stratagene MX-4000 multiplex quantitative PCR system. ROX (Stratagene) was used as reference dye. The PCR conditions (final reaction volume of 25 µl) were as follows: 0.5 µl cDNA template, 300 nmol l^{-1} forward and reverse primer, 12.5 µl 2× Master Mix, 1:30000 final dilution of ROX. The annealing and extension temperatures over 40 cycles were 58°C (30 s) and 72°C (30 s), respectively. All the primers used for real-time PCR (including the reference gene β-actin) were designed using Primer3 software (http://www-genome.wi.mit.edu/cgi-bin/primer/primer3_www.cgi; Table 1). The specificity of the primers was verified by cloning (TOPO TA cloning kit; Invitrogen) and sequencing of amplified products. The construction of SYBR Green dissociation curves after completion of 40 PCR cycles revealed the presence of single amplicons for each primer pair. To ensure that residual genomic DNA was not being amplified, control experiments were performed in which reverse transcriptase was omitted during cDNA synthesis. Relative expression of mRNA levels was determined (using β-actin as an endogenous standard; GenBank accession no. BC063950.1) by a modification of the ΔΔCt method (Pfaffl, 2001). Amplification efficiencies were determined from standard curves generated by serial dilution of plasmid DNA, and varied between ~90 and ~110%.

Probe synthesis for *in situ* hybridization

Primers were designed to produce probes of 748, 486 and 805 base pairs for *za3*, *za4* and *za6c*, respectively (Table 1) using plasmid DNA as template. An aliquot of the PCR products was run on a 1.25% gel and the rest was purified using a PCR purification kit (Sigma). The purified product was cloned in PCR II vector (Invitrogen) and the desired clone was purified using a plasmid miniprep purification kit (Sigma). The purified plasmid DNA was sequenced using M13 forward (–20) and M13 reverse primers to confirm identity and determine the orientation of the cloned sequence within the vector. To obtain linear DNA flanked by SP6 and T7 promoters, M13 forward (–20) and M13 reverse primers were used to amplify the inserted probes. Sense and antisense DIG-labeled RNA probes were synthesized using 1 µg of purified PCR product in the *in vitro* transcription reaction using the appropriate SP6 or T7 RNA polymerase (New England Biolabs) for 1 h at 37°C.

In situ hybridization

Larvae were placed in 4% PFA (pH 7.4) at 4°C overnight before being washed (2× 5 min) with PBS and dehydrated by methanol washes (CH_3OH): 2× 5 min at room temperature followed by 1× 60 min at –20°C. Following dehydration, embryos were rehydrated in a graded series of CH_3OH–PBS washes: 1× 5 min in 75% CH_3OH–25% PBS, 1× 5 min in 50% CH_3OH–50% PBS, 1× 5 min in 25% CH_3OH–75% PBS, 3× 5 min in 100% PBST (1× PBS, 0.1% Tween 20).

Embryos were rinsed in 4 ml of 20 mg ml^{-1} of Proteinase K (Invitrogen) for 10 min at room temperature (RT) before they were washed 1× 5 min in PBST and fixed for 20 min in 4% PFA–PBS. The hybridization mix (Hyb-mix) for use in prehybridization, hybridization and washes was prepared as follows: 5.0 ml formamide, 2.5 ml 20× SSC, 50 µl of 20% Tween 20, 5 mg ml^{-1} heparin, 92 µl 1 mol l^{-1} citric acid, H_2O to final volume of 10 ml. For prehybridization and hybridization, 100 mg ml^{-1} yeast tRNA was added to the Hyb-mix.

Larvae were prehybridized for 2–3 h in 200 ml Hyb-mix at 65°C. For hybridization, 200 ml of Hyb-mix containing 1 ml of probe was added to the embryos and they were left overnight at 65°C. Embryos were then washed as follows: 10 min in 75% Hyb-mix–25% 2× SSC at 65°C; 10 min in 50% Hyb-mix–50% 2× SSC at 65°C; 10 min in 25% Hyb-mix–75% 2× SSC at 65°C; 10 min in 100% 2× SSC at 65°C; 2×30 min in 0.2× SSC at 60°C; 5 min in 75% 0.2× SSC–25% PBST at RT; 5 min in 50% 0.2× SSC–50% PBST at RT; 5 min in 25% 0.2× SSC–75% PBST at RT; 5 min in PBST at RT.

Following washes, the larvae were pre-incubated for 1 h in PBST containing 2% calf serum and 2 mg ml^{-1} BSA and were then incubated with 1:2500 anti-DIG antibody (Roche) for 2–4 h at RT with gentle shaking. Following incubation, embryos were washed (6× 15 min in PBST) and placed in staining buffer (100 mmol l^{-1} Tris pH 9.5, 50 mmol l^{-1} $MgCl_2$, 100 mmol l^{-1} NaCl, 0.1% Tween 20, 1 mmol l^{-1} levamisol) for 5 min. 14 µl of 5-bromocresyl-3-indolyl phosphate (BCIP; Fisher, Ottawa, Ontario, Canada; BCIP stock solution was 50 mg ml^{-1} in dimethylformamide) and 27 µl of nitroblue tetrazolium (NBT; Sigma; NBT stock solution was 50 mg

in 0.7 ml dimethylformamide + 0.3 ml H_2O) were added to the staining buffer and embryos were stained for up to 2 h or until satisfactory coloration occurred. The embryos were then washed 2× 5 min in PBST at RT.

The larvae were examined using a Nikon Eclipse E600 light microscope combined with a Nikon Plan Fluor 20× dry objective lens (numerical aperture 0.50). Images were taken using QImaging MicroPublisher 5.0 digital microscope camera and QCapture v2.68.

Western blotting

Proteins were prepared from fresh tissues by homogenization on ice in 1:5 w/v of extraction buffer containing 50 mmol l^{-1} Tris-HCl, 150 mmol l^{-1} NaCl, 1% NP-40, 0.5% sodium deoxycholate, 2 mmol l^{-1} sodium fluoride, 2 mmol l^{-1} EDTA, 0.1% SDS, and protease inhibitor cocktail (Roche). The samples were incubated on ice for 10 min and briefly sonicated to break up any DNA that might have been extracted. The samples were centrifuged at 16,000 ***g*** for 20 min at 4°C and the supernatants were stored at –20°C before use. Samples were size fractionated by reducing SDS-PAGE using 10% separating and 4% stacking polyacrylamide gels and transferred to nitrocellulose membranes (Bio-Rad, Mississauga, ON, Canada). After transfer, each membrane was blocked for 2 h in 5% milk powder–TBS-T (1× TBS, 0.1% Tween 20) and then incubated (1:5000 dilution) for 3 h at RT with a polyclonal affinity-purified rabbit primary antibody custom produced (Abgent; San Diego, CA, USA) against a synthetic peptide (AEQHERINRKRKTLR) corresponding to amino acids 21–35 of zSLC26A3 (accession no. ACI05561). The membranes were washed (4× 5 min) in PBS and incubated for 1 h at RT with peroxidase-conjugated secondary anti-rabbit Ig (1:25000). The specific bands were detected by enhanced chemiluminescence (ECL; Pierce; SuperSignal West Pico Chemiluminescent Substrate, Rockford, IL, USA). The protein size marker used was obtained from Fermentas Life Sciences. Antibodies were also produced against zSLC26A4 and A6c but these did not produce satisfactory results.

Immunocytochemistry

Larvae were killed with an anesthetic (MS-222) overdose and incubated for 20 min at 4°C in a solution of 4% paraformaldehyde (PFA; prepared in PBS, pH 7.4). They were then washed with PBS (3× 5 min) and treated with 100% ethanol at –20°C for 10 min. Larvae were rinsed again with PBS (3× 5 min) and subsequently blocked with 3% bovine serum albumin (BSA) in PBS for 1 h before being washed again with PBS (3× 5 min). Larvae were incubated for 2 h at RT with 1:100 PBS-diluted primary ZA3 antibody. Several of the larvae were co-incubated with 1:100 α5, a mouse monoclonal antibody directed against Na^+/K^+-ATPase of chicken, or ZN-12, a zebrafish-derived neuron-specific marker (Trevarrow et al., 1990). ZN-12 and α5 were obtained from the Developmental Studies Hybridoma Bank (University of Iowa, USA).

Larvae were washed (3× 5 min) with PBS before being incubated for 1 h with 1:400 Alexa-Fluor-546 anti-rabbit and 1:400 Alexa-Fluor-488 anti-mouse (Molecular Probes, Burlington, ON, Canada). The larvae were then washed again (3× 5 min) in PBS and whole-mount preparations were examined with a confocal scanning system (Olympus BX50WI, Melville, NY, USA) equipped with an argon laser. Images were collected using Fluoview 2.1.39 graphics software (Fluoview, Melville, NY, USA).

Morpholino gene knockdown

Morpholino oligonucleotides (MOs) complementary to the translational start site of *za3*, *za4* and *za6c* were microinjected into one-cell stage embryos. Injection needles were pulled from filamented 1.0 mm borosilicate glass (Sutter Instrument, Novato, CA, USA) and the injections were controlled with an IM 300 programmable microinjector (Narishige, East Meadow, NY, USA). MOs (GeneTools) used were as follows: *za3*, [5′-ATGCAG-CCTTTCGGCAGACACTATG-3′]; *za4*, [5′-ATGGCGATAC-ATCTTGTGGAGTACG-3′]; *za6c*, [5′-GAGAGAATGGATTC-AAGACATGAAG-3′]; and a standard control, [5′-CCTCTTA-CCTCAGTTACAATTTATA-3′]. MOs were diluted to working standards of 4 ng ml^{-1} in Danieau buffer (58 mmol l^{-1} NaCl, 0.7 mmol l^{-1} KCl, 0.4 mmol l^{-1} $MgSO_4$, 0.6 mmol l^{-1} $Ca(NO_3)_2$, 5 mmol l^{-1} Hepes, pH 7.6) and 0.05% Phenol Red. Embryos were injected with approximately 1 nl of the MO–Danieau buffer solution.

The gene-specific MOs were tagged with carboxyfluorescein at the 3′ ends, allowing the injected embryos to be screened for MO uptake with a Nikon SMZ1500 (Nikon, Mississauga, Ontario, Canada) fluorescence dissecting microscope. Any embryos not exhibiting widespread fluorescence 24 h post-injection were discarded.

To test for efficacy of the *za3*, *za4* and *za6c* morpholinos, fusion constructs were made in which the *za3*, *za4* and *za6c* MO target sequences were separately introduced upstream of and in frame with the red fluorescent protein dTomato (Shaner et al., 2004) coding sequence. Embryos were injected with *in vitro*-synthesized zA-dTomato mRNA alone or together with each of the zA MOs (only one MO was co-injected into each embryo).

Chloride flux measurements

Tracer medium was prepared by adding 0.13 μCi $^{36}NaCl$ (American Radiolabeled Chemicals, MO, USA) to 500 μl of standard zebrafish water (Westerfield, 2007). Five embryos or larvae were pooled and exposed to the medium for 2 h. Water samples were collected at the beginning and the end of exposure for Cl^- concentration measurement. After 2 h incubation, embryos were briefly rinsed with isotope-free water, gently blotted dry, weighed and digested overnight in 100 μl of NCS-II tissue solubilizer (GE Healthcare, Piscataway, NJ, USA) at 42°C. After neutralization with glacial acetic acid, the digested solution was mixed with 10 ml of scintillation cocktail (Bio Safe II; Research Products International, Mt. Prospect, IL, USA). Incorporated radioactivity (in d.p.m. after quench correction) was determined using a liquid scintillation beta counter (Beckman LS-6500). The rate of chloride influx (J_{in}; in pmol mg^{-1} h^{-1}) was calculated using:

$$J_{in} = Q_{embryo} X_{out}^{-1} t^{-1} W^{-1},$$

where Q_{embryo} is the incorporated radioactivity (c.p.m. mg^{-1}), X_{out} is specific activity of medium (d.p.m. $pmol^{-1}$), t is length of incubation (h) and W is total wet mass of embryos (mg).

Acid–base excretion measurements

Larval (4 d.p.f.) zebrafish (3–5 larvae per experiment for N=1) were placed in 15 ml HCO_3^- free control water (reconstituted from reverse osmosis water) in a titration vessel (Radiometer Analytical, London, Ontario, Canada; PP.22–45 ml). The water was constantly aerated with atmospheric air using PE50 tubing to aid in mixing. A pH electrode (model PHC4000.8; Radiometer) and a microburette tip, both of which were attached to a pH-stat titration system (model TIM 854 or 856; Radiometer), were positioned just below water level into the titration vessel. The pH-stat titrations were performed at pH 6.800 throughout all experiments, with pH values and rate of acid addition logged on personal computers using Titramaster software (versions 1.3 and 2.1 OR 85). Generally, water pH was

maintained within ±0.003 pH unit around the set point throughout the experiments. Base secretion rates were calculated from the rate of addition and concentration of titrant (0.0005 mol l^{-1} HCl). Water samples were taken for determination of ammonia excretion rates using a colorimetric assay (Verdouw et al., 1978). Net acid excretion (J_{NET}^{H+}) was calculated as described by McDonald and Wood (McDonald and Wood, 1981).

Statistical analysis

Data are shown in figures as means ±1 standard error of the mean. Real-time PCR data were analyzed using a one-sample *t*-test to determine whether relative mRNA levels were greater than 1. All other data were analyzed by two-way analysis of variance (ANOVA) or one-way ANOVA (base excretion data; Fig. 11). In cases where the ANOVA indicated statistical differences, the data were further analyzed using a Bonferroni multiple comparison test (all pairwise comparisons). In all cases, the fiducial limit of significance was set at 5%.

RESULTS

A phylogenetic analysis of the SLC26 gene family produced well supported trees of similar topology from both the NJ (Fig. 1) and MP methods. Zebrafish SLC26A3 grouped with other vertebrate SLC26A3 sequences, with the closest relative being the *T. obscurus* SLC26A3. Similarly, SLC26A4 grouped with other vertebrate SLC26A4 sequences. Interestingly, a *X. laevis* sequence that had been denoted as an SLC26A3 protein grouped within the SLC26A4 group, suggesting this protein is actually a second *X. laevis* SLC26A4 protein. The zebrafish SLC26A6c sequence obtained in the current study also grouped with other vertebrate SLC26A6 sequences, specifically with the fish SLC26A6c proteins, and has been denoted as such. Interestingly, the various fish SLC26A6 isoforms (A6a–A6c) all group together, and independently of the tetrapod SLC26A6 isoforms (A6a–A6d). This suggests that the common vertebrate ancestor had only a single SLC26A6 gene, and evolved multiple copies after the divergence of fish and tetrapods. It is unclear how many SLC26A6 isoforms are found in tetrapod vertebrates, with as many as four being found in humans, but fish species appear to contain at least three, although four are found in zebrafish. It also appears that *O. beta* may be unique in that it has a duplication of the A6a isoform. Furthermore, it should be noted that a single zebrafish SLC26A6 sequence (no additional isoform designation) is basal to both the tetrapod and fish SLC26A6 groups, which may represent an ancestral SLC26A6 ortholog.

Representative micrographs obtained from *in situ* hybridization on whole-mount larvae (7 d.p.f.) are depicted in Fig. 2. *slc26a3* mRNA appeared to be most abundant in the heart, mesonephros, neuromasts and gill (Fig. 2A). For *slc26a4* mRNA, the predominant sites of expression appeared to be the heart and mesonephros (Fig. 2B). A similar pattern of expression was observed for *slc26a6c* with obvious localization to the mesonephros and mesonephric duct (Fig. 2C). No staining was observed using a sense zA4 probe (Fig. 2D).

Although polyclonal antibodies were generated for the three SLC26 proteins described in this paper, only the one raised against zSLC26A3 proved to be useful for immunocytochemistry. On western blots, the antibody yielded a single band of approximately 80 kDa (Fig. 3D) which was not observed when using the pre-immune serum or after pre-absorption of antibody with excess peptide antigen. The estimated molecular mass of 80 kDa is similar to the predicted mass of the ALC26A3 protein (83 kDa). Overall however, the antibody proved difficult to work with and required

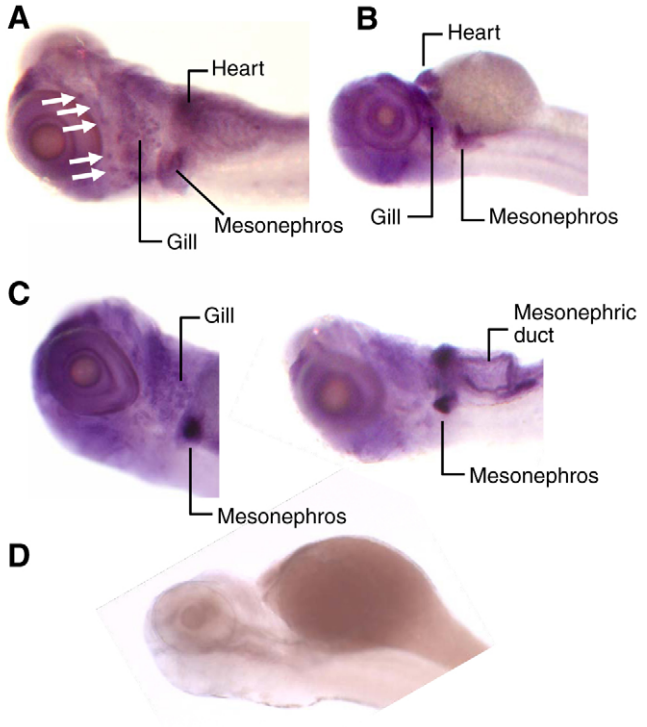

Fig. 2. Representative micrographs of whole-mount *in situ* hybridization using antisense probes against (A) *slc26a3*, (B) *slc26a4* and (C) *slc26a6c*. The arrows in A indicate neuromasts. (D) No staining was observed when a sense probe (*zA4*) was used.

the use of extremely sensitive chemiluminescence detection kits. An analysis of numerous whole-mount specimens, ranging from 3–9 d.p.f., revealed several patterns of SLC26A3 immunoreactivity that are depicted in Fig. 3. The neural masts of the lateral line system exhibited marked immunoreactivity (Fig. 3A). Aside from the neural masts, the most common observation was the presence of a modest number (less than 10%) of SLC26A3-positive cells that were scattered among the more prevalent NKA-positive cells dispersed along the developing gill arches (Fig. 3B). In some instances, SLC26A3 was colocalized with Na^+/K^+-ATPase (Fig. 3C) whereas in some cells expressing SLC26A3, there was no apparent Na^+/K^+-ATPase immunoreactivity (Fig. 3D). SLC26A3-positive cells were never observed on the yolk sac or skin of the body. In contrast to the results of *in situ* hybridization, zA3 protein immunoreactivity was not apparent in the heart or mesonephros, possibly a reflection of insufficient antibody penetration into these deeper lying tissues (e.g. compared to epithelial cells).

The effects of developmental age (1 hpf–30 d.p.f.) on the relative expression of SLC26 mRNAs are depicted in Fig. 4. There was an obvious transient increase in mRNA expression of *za3*, *za4* and *za6c* at 5–10 d.p.f.; additionally, *zA4* was significantly elevated at 4 d.p.f. (Fig. 4). The changes in abundance of SLC26 mRNAs were not a result of marked changes in the reference gene β-actin because average Ct values for this gene varied little between 1 hpf and 15 d.p.f. (20.1±0.5–21.8±0.4) in comparison with the genes of interest. At 30 d.p.f. and in adults (>3 months), the Ct values for β-actin were reduced to 18.5±0.5 and 17.8±0.3, respectively, which may have influenced the relative mRNA expression data.

$J_{in}^{Cl^-}$ increased rapidly with developmental age from 12.9±1.6 pmol mg^{-1} h^{-1} at 1 d.p.f. to 281.8±27.9 pmol mg^{-1} h^{-1} at 5 d.p.f. (Fig. 5A); from 5–10 d.p.f., $J_{in}^{Cl^-}$ was more-or-less constant

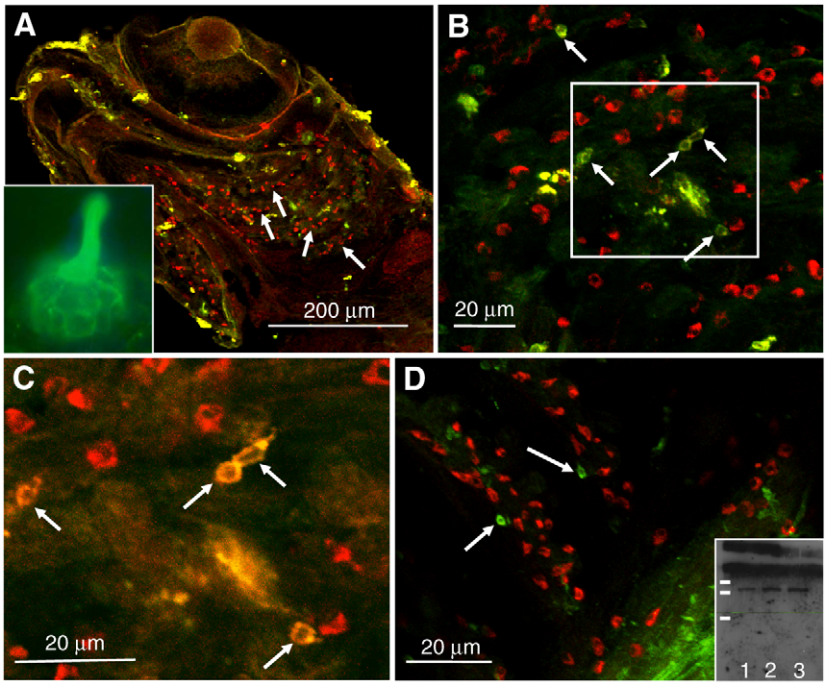

Fig. 3. Representative laser scanning confocal micrographs illustrating the presence and distribution of SLC26A3 (green) and Na^+/K^+-ATPase (NKA; red) immunoreactive cells in the head and gill regions of zebrafish larvae at 6–9 d.p.f. (A) Low magnification image demonstrating strong SLC26A3 immunoreactivity of the neural masts (a high magnification view is shown in the inset), abundance of NKA-positive cells distributed along the developing gill arches (arrows) and a few sparsely distributed SLC26A3-positive cells. (B) A higher magnification image of a different specimen demonstrating the relative scarcity within the developing gills of SLC26A3-positive cells (arrows) in comparison to NKA-positive cells. (C) A second and higher magnification image of an area of gill from B (outlined with box), using different laser intensity settings, illustrates colocalization of SLC26A3 and NKA in a subset of gill cells (arrows). (D) Two developing gill arches exhibit an abundance of NKA-positive cells but only two obvious SLC26A3-positive cells (arrows) that are not enriched with NKA. The inset in D is a representative western blot showing the presence of a single immunoreactive band at approximately 80 kDA in three separate pools of protein (lanes 1–3). The size markers correspond to 95, 72 and 55 kDa.

(no statistical differences). The marked increase in $J_{in}^{Cl^-}$ from 2–3 d.p.f. was not a result of hatching because the dechorionated embryos demonstrated a similar rise in $J_{in}^{Cl^-}$ at this stage of development (Fig. 5B). In both the intact and dechorionated fish, prior rearing in low [Cl^-] water resulted in a significant stimulation of $J_{in}^{Cl^-}$ (Fig. 5). Increased rates of $J_{in}^{Cl^-}$ in the fish reared in low [Cl^-] water were associated with increased levels of SLC26 mRNA after 4 d.p.f.; for *za3* and *za6c*, statistically significant differences were observed at 4–7 d.p.f. whereas for *za4*, increased expression was only detected at 10–15 d.p.f. (Fig. 6). Fish reared in high Cl^- water exhibited an unaltered pattern of mRNA expression with development (Fig. 6).

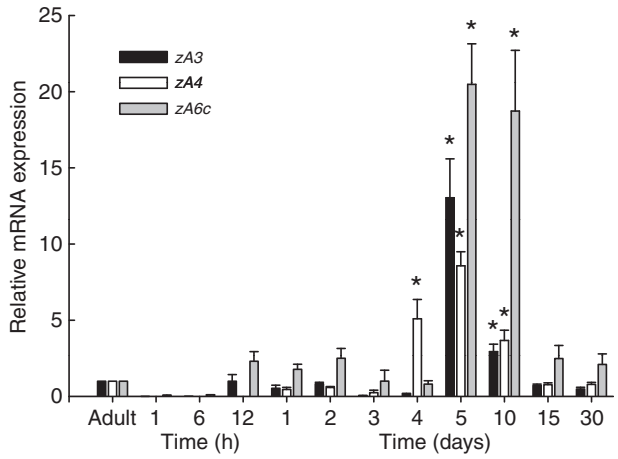

Fig. 4. The expression of mRNA for zebrafish SLC26 genes (*zA3*, *zA4* and *zA6c*) during development as determined by real time RT-PCR. The data (N=4 for each gene) are presented relative to adult whole body levels (assigned a value of 1) after normalization to β-actin. Asterisks indicate data points that are statistically greater than one (one-sample t-test; P<0.05). Note that the x-axis is not drawn to scale and that data for *zA4* mRNA were not obtained at 1–12 h. Data are means ± 1 s.e.m.

The interactive effects of selective SLC26 gene knockdown and ambient Cl^- levels on rates of $J_{in}^{Cl^-}$ are depicted in Fig. 7. The embryos injected with zA–dTomato mRNA alone exhibited ubiquitous expression. However, no dTomato expression was observed when the corresponding SLC26 MO was injected into the embryos along with or after zA–dTomato mRNA injection, which indicates that the SLC26 morpholinos can effectively block the translation of zA-dTomato and are, therefore, able to recognize and block translation of the target sequence *in vivo*.

Although successful knockdown appeared to be achieved for each gene (based on the presence or absence of red fluorescence; see above), a significant reduction of $J_{in}^{Cl^-}$ under normal rearing conditions was observed only for fish experiencing *za3* knockdown (Fig. 7A). Under condition of low ambient [Cl^-], $J_{in}^{Cl^-}$ was reduced significantly by all morpholinos (Fig. 7A–C). In fish reared under high environmental [Cl^-], $J_{in}^{Cl^-}$ was unaffected by SLC26 gene knockdown.

Raising fish in water containing high levels of $NaHCO_3$ (Fig. 8A, Fig. 9) or exposing them to elevated $NaHCO_3$ for 24 h at 7 d.p.f. (Fig. 8B) resulted in significant increases in the rates of $J_{in}^{Cl^-}$. The increases in $J_{in}^{Cl^-}$ with base exposure were prevented or diminished by SLC26 morpholino knockdown (Fig. 10). Knockdown of *za3* produced the greatest effect (Fig. 10A) whereas knockdown of *za4* (5 mmol l^{-1} $NaHCO_3$ only; Fig. 10B) or *za6c* (2 mmol l^{-1} $NaHCO_3$ only; Fig. 10C) caused smaller changes.

Whole body base excretion in 5–7 d.p.f. larvae was significantly reduced by morpholino knockdown of *zA3* or *zA6c* (Fig. 11).

DISCUSSION

A critique of the methods

The use of morpholino antisense oligonucleotides to achieve transient gene knockdown in developing zebrafish (Nasevicius and Ekker, 2000) has emerged as an important tool to assess physiological functions, including mechanisms of transepithelial ion and ammonia transport (Pan et al., 2005; Horng et al., 2007; Lin et al., 2008; Shih et al., 2008; Braun et al., 2009; Tseng et al., 2009; Chang et al., 2009). In their recent review on the use

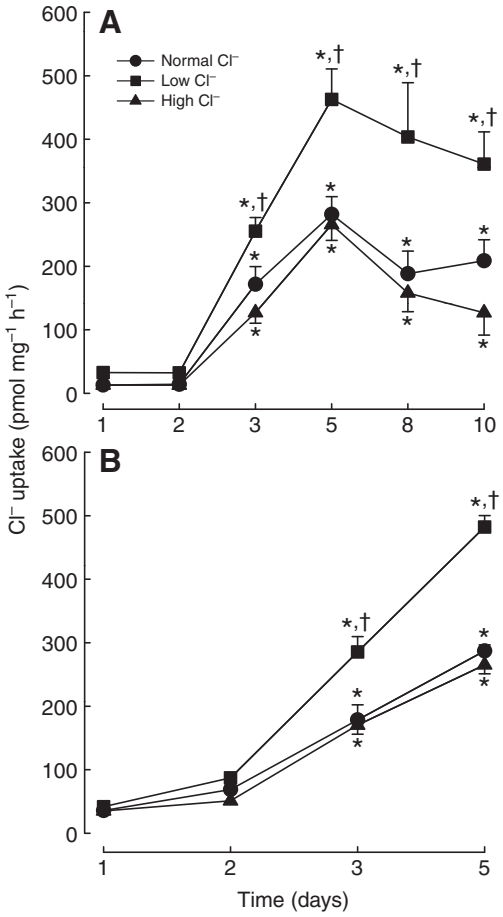

Fig. 5. The interactive effects of developmental age and rearing Cl^- levels on Cl^- uptake ($J_{in}^{Cl^-}$) in (A) intact and (B) dechorionated (at 2 d.p.f.) zebrafish (*Danio rerio*). $J_{in}^{Cl^-}$ increased (asterisks, $P<0.05$) from 2 to 5 d.p.f. and thereafter remained more-or-less constant. Fish raised in low ambient [Cl^-] (filled squares; $N=6$) exhibited increases in $J_{in}^{Cl^-}$ (daggers; $P<0.05$) at 3–10 d.p.f. when compared with fish raised in normal ambient [Cl^-] (filled circles; $N=6$) or high ambient [Cl^-] (filled triangles; $N=6$). Similar data were obtained from the dechorionated fish (B; $N=4$ for each ambient [Cl^-] between 2 and 5 d.p.f.). Data are means ± 1 s.e.m.

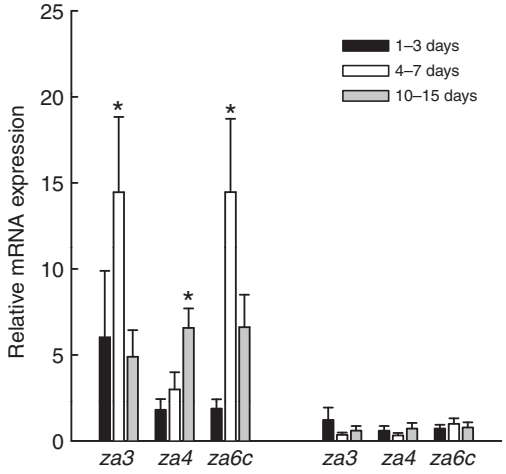

Fig. 6. The effects of rearing zebrafish under conditions of low or high ambient [Cl^-] on the relative mRNA expression of three SLC26 genes (*za3*, *za4* and *za6c*). All data were compared with mRNA levels obtained from fish reared in control water ,which were assigned values of 1. Asterisks indicate values greater than 1 (one-sample *t*-test; $P<0.05$). Because of low sample numbers, data were pooled for 1–3 d.p.f. ($N=12$), 4–7 d.p.f. ($N=8$) and 10–15 d.p.f. ($N=8$).

of antisense technologies in gene knockdown experiments, Eisen and Smith (Eisen and Smith, 2008) highlighted three important issues that should be considered in such studies. First, evidence should be provided that targeted gene knockdown is indeed occurring. Second, when using multiple morpholinos targeted against several paralogs of a multi-gene family, their specificity needs to be established and third, the possibility that off target effects might be accounting for observed phenotypes should be considered.

The most convincing method to verify knockdown is to directly assess protein levels in sham- and morpholino-injected fish by western blotting. Unfortunately, this technique requires the procurement of appropriate antibodies able to recognize zebrafish-specific proteins. In the course of the present study, we developed three homologous antibodies against the three SLC26 gene products under investigation (zA3, zA4 and zA6c). However, because only one of the antibodies (to zA3) proved useful, we chose another strategy commonly used to assess the efficacy of knockdown, in which embryos are co-injected with a fluorescent fusion construct (Eisen and Smith, 2008). The results of these experiments revealed a complete absence of fluorescence for up to 7 d.p.f. in fish co-injected with morpholinos. Moreover, using this approach we were able to confirm specificity of the morpholino oligonucleotides because fluorescence was prevented only in those embryos that were co-injected with the corresponding morpholino (e.g. co-injection of SLC26A3 fusion construct and SLC26A3 morpholino). The specificity of the morpholinos was not surprising given that the maximum number of identical nucleotides between any two morpholinos was 7/24. Two other strategies employed to minimize the chances of off target effects are the use of two or more morpholinos against any single gene target and RNA rescue in which a form of the target RNA (not recognizable by the morpholino) is co-injected in an attempt to re-establish the control phenotype. Neither of these approaches was used in the present study owing, in part, to diminishing isotope resources. Indeed, we are unaware of any isotope provider currently able to supply ^{36}Cl to North American researchers.

SLC26 Cl^-/HCO_3^- exchangers appear to mediate Cl^- uptake in zebrafish larvae

The previous evidence implicating Cl^-/HCO_3^- exchange as a mechanism for Cl^- uptake in freshwater fish is overwhelming (Krogh, 1937; Krogh, 1938; Maetz and Garcia Romeu, 1964; De Renzis and Maetz, 1973; De Renzis, 1975; Braun et al., 2009) (reviewed by Marshall, 1995; Claiborne, 1998; Evans et al., 1999; Marshall, 2002; Perry et al., 2003a; Perry et al., 2003b; Evans et al., 2005; Perry and Gilmour, 2006; Marshall and Grosell, 2006; Tresguerres et al., 2006; Hwang and Lee, 2007; Evans, 2008). Prior to the demonstration of pendrin (SLC26A4)-like immunoreactivity on the elasmobranch gill (Piermarini et al., 2001), it was generally considered that branchial Cl^-/HCO_3^- exchange was accomplished by one or more members of the SLC4 gene family. This conclusion was reinforced by the results of studies utilizing immunocytochemistry (Wilson et al., 2000), *in situ* hybridization (Sullivan et al., 1996) and data obtained from pharmacological

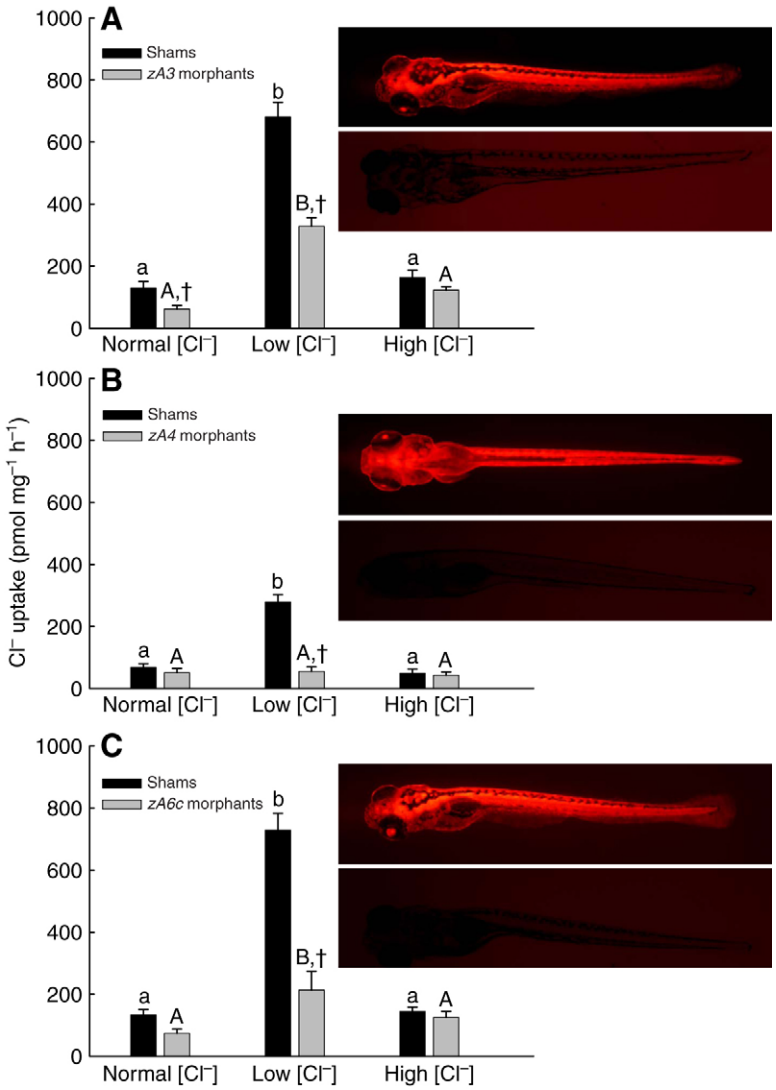

Fig. 7. The effects of antisense oligonucleotide morpholino knockdown of (A) *slc26a3*, (B) *slc26a4* or (C) *slc26a6c* on chloride uptake ($J_{in}^{Cl^-}$) in 5 d.p.f. zebrafish larvae reared in control water or in water containing low or high [Cl^-]. The insets in each panel are representative images of fish at 7 d.p.f. previously injected at the one-cell stage with 100 pg of SLC26 mRNA – red fluorescent constructs in the absence or presence of the respective morpholinos (4 ng). The absence of red fluorescence in the fish injected with morpholinos indicates successful gene knockdown. Differences between morpholino- and sham-injected fish are indicted by daggers (P<0.05). Differences within either the sham- or morpholino-injected fish as a function of ambient [Cl^-] are indicated by dissimilar letters (lower case for shams; upper case for morphants).

studies employing the Cl^-/HCO_3^- exchange blockers SITS/DIDS or SCN^- (Epstein et al., 1973; Perry and Randall, 1981; Perry et al., 1981a; Chang and Hwang, 2004; Preest et al., 2005). With the benefit of hindsight, however, the results of these former studies are subject to reinterpretation. For example, the 24-mer *in situ* probe used by Sullivan et al. (Sullivan et al., 1996), although homologous with rat *AE1* (*SLC4A1*) (Kudrycki and Shull, 1989) shares 63–71% sequence identity with *zslc26a3*, *za4* and *za6c* and thus may have hybridized to multiple mRNA targets including members of the SLC26 gene family. In addition, disulfonic stilbene derivatives including SITS and DIDS are not specific blockers of SLC4 anion exchangers but also block members of the SLC26 gene family (Soleimani et al., 2001). Finally, the antibody used by Wilson et al. (Wilson et al., 2000) was generated against denatured rainbow trout (*Oncorhynchus mykiss*) red blood cell SLC4A1 protein (Cameron et al., 1996) and thus its specificity for SLC4A1 *versus* other SLC4 and SLC26 proteins cannot be easily confirmed by sequence analysis.

Although we cannot exclude the possibility that SLC4 genes are also involved, the results of the present study using a combination of approaches, including gene knockdown, provide evidence for the involvement of SLC26 gene family members in Cl^- uptake in zebrafish larvae. Indirect evidence was provided by the increased expression of SLC26 mRNA in larvae exposed to water containing low ambient [Cl^-] or elevated [HCO_3^-], conditions which markedly increased rates of whole body Cl^- uptake. Direct evidence was provided by the demonstration of significantly reduced rates of Cl^- uptake and base excretion in fish experiencing *za3* knockdown while being raised in control water and a significant attenuation of the stimulatory effects of prior exposure to low ambient [Cl^-] or elevated ambient [HCO_3^-] (*za3* and *za6c* only) on Cl^- uptake. The effects of low ambient [Cl^-] on increasing Cl^- uptake capacity was reported previously for adult zebrafish (Boisen et al., 2003) and tilapia [*Oreochromis mossambicus* (Chang et al., 2003)]. We (S.F.P. and M.B., unpublished data) recently demonstrated that adult zebrafish exposed to water of low ambient [Cl^-] exhibit increased branchial expression of SLC26A3, A4 and A6c mRNA thereby suggesting that at least in zebrafish, the increase in Cl^- transport capacity [as indicated by a threefold increase in $J_{MAX}^{Cl^-}$ (Boisen et al., 2003)] reflects an increased expression of branchial SLC26 genes. Although not measured in the present study, we have assumed that, as in rainbow trout (Perry et al., 1981), the addition of HCO_3^- to the water causes metabolic alkalosis. Thus, we believe that the increased expression of SLC26 mRNA in fish during exposure to high ambient [HCO_3^-] was a compensatory response aimed at increasing rates of Cl^-/HCO_3^- exchange.

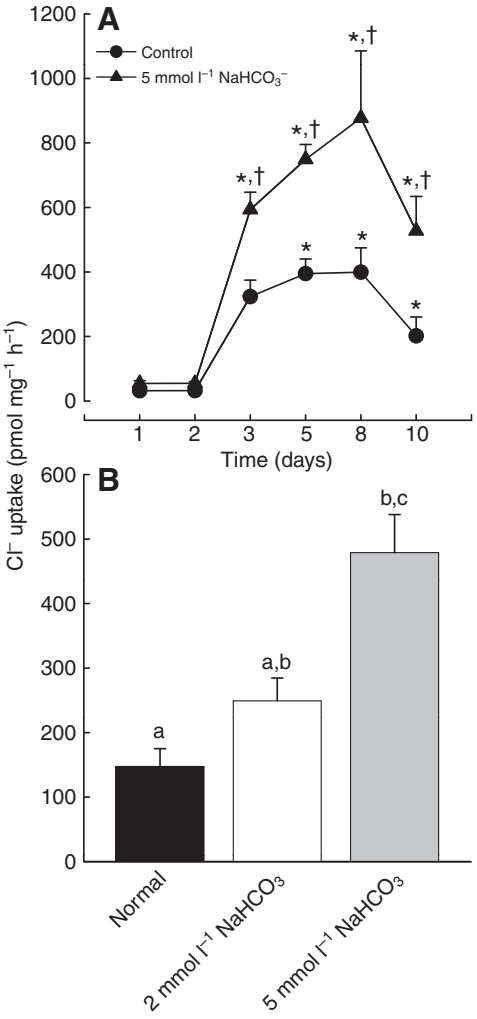

Fig. 8. (A) The time-dependent effects of rearing fish in elevated ambient [$NaHCO_3$] (5 mmol l^{-1}) or (B) the effects of a 24 h incubation of 7 d.p.f. larvae with 2 or 5 mmol l^{-1} external $NaHCO_3$ on Cl^- uptake in zebrafish (*Danio rerio*). For A, significant differences within either the control (N=5 at each time point) or the 5 mmol l^{-1} $NaHCO_3$ group (N=5 at each time point) are denoted by asterisks (P<0.05); differences between the control fish and those reared in elevated $NaHCO_3$ are indicated by daggers (P<0.05). In B, significant differences are denoted by dissimilar letters (N=6, 4 and 6 for the controls, 2 mmol l^{-1} and 5 mmol l^{-1} groups, respectively).

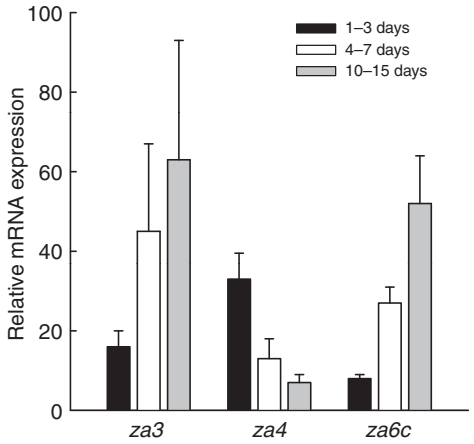

Fig. 9. The effects of rearing zebrafish (*Danio rerio*) under conditions of high ambient [$NaHCO_3$] on the relative mRNA expression of three SLC26 genes (*zA3*, *zA4* and *zA6c*). All data were compared to mRNA levels obtained from fish reared in control water, which were assigned values of 1. Asterisks indicate values greater than 1 (one-sample *t*-test; P<0.05). Because of low sample numbers, data were pooled for 1–3 d.p.f. (N=10), 4–7 d.p.f. (N=10) and 10–15 d.p.f. (N=6).

Which cell types are responsible for Cl^-/HCO_3^- exchange in developing zebrafish?

The results of previous studies examining ionic uptake in developing zebrafish embryos and larvae have implicated ionocytes of the yolk sac and skin as sites of Ca^{2+} (Pan et al., 2005) and Na^+ uptake (Yan et al., 2007) (reviewed by Hwang and Lee, 2007). For Ca^{2+} uptake, the participating ionocyte subtypes are believed to be mitochondrion rich (MR) cells enriched with Na^+/K^+-ATPase (NaR cells) whereas for Na^+ uptake, the participating subtypes are thought to be MR cells enriched with apical V-type H^+-ATPase [HR cells (Hwang and Lee, 2007)]. Thus, we had anticipated that the results of the *in situ* hybridization and immunocytochemistry (SLC26A3 only) experiments would also reveal the presence of SLC26 mRNA or protein within ionocytes of the yolk sac and skin. However, in contrast to expectations, we were unable to detect SLC26 mRNA on the yolk sac or skin up to 9 d.p.f. Instead, SLC26 mRNA appeared to be localized to the mesonephros and/or mesonephric ducts, heart (*za3* and *za4*), neuromasts (*za3*) and gills (Fig. 2). The immunocytochemistry results demonstrated that a subset of branchial MR cells exhibited SLC26A3 immunoreactivity. The apparent absence of SLC26 Cl^-/HCO_3^- transporters on the yolk sac and skin noted in this study obviously is inconsistent with the prevailing view that ionic uptake in developing fish occurs predominantly across the skin prior to maturation of the gills (reviewed by Varsamos et al., 2005). However, ionocytes are clearly present within the gill arches of larval zebrafish (Fig. 3) and as in other species (Varsamos et al., 2005), they appear well before the development of lamellae (Rombough, 2002; Rombough, 2007). Thus, it is conceivable that Cl^- uptake in larval zebrafish is mediated by SLC26 Cl^-/HCO_3^- exchangers restricted to a subset of ionocytes of the gill. Some of these ionocytes were also enriched with Na^+/K^+-ATPase but others were not.

Previous experiments have provided indirect evidence that branchial ionocytes (also referred to as MR cells or FW chloride cells) are responsible for Cl^- uptake in adult FW fish. For example, in brown trout (*Salmo trutta*), the intracellular concentration of chlorine within branchial MR cells is affected by ambient Cl^- levels (Morgan et al., 1994) or external application of the Cl^- uptake inhibitor thiocyanate (Morgan and Potts, 1995); the pavement cells were unaffected. In rainbow trout (Goss and Perry, 1993; Perry and Goss, 1994), brown bullhead (*Ictalurus nebulosus*) (Goss et al., 1992; Goss et al., 1994) and tilapia (*Oreochromis mossambicus*) (Chang et al., 2003), the rates of Cl^- uptake (and in some cases base excretion) are significantly correlated with the numbers of MR cells in contact with the water. In light of the finding of specific subtypes of MR cells (Pisam et al., 1987; Chang et al., 2001; Goss et al., 2001; Hiroi et al., 2005; Laurent et al., 2006), models have been developed in which specific functions are assigned to the various MR cell types. By analogy with the β-intercalated cell of the mammalian renal collecting duct, one of the branchial MR cell subtypes is thought to function as a base-secreting cell with an apical membrane Cl^-/HCO_3^- exchanger and a basolateral V-type H^+-ATPase (Piermarini et al., 2002). Thus, we propose that the SLC26

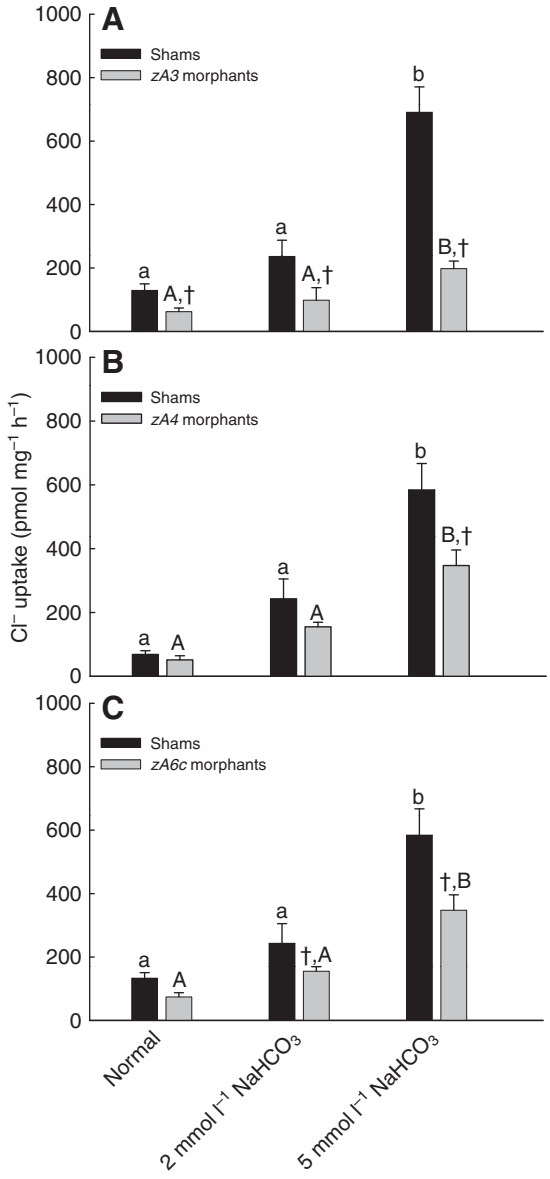

Fig. 10. The effects of antisense oligonucleotide morpholino knockdown of (A) *SLC26A3*, (B) *SLC26A4* or (C) *SLC26A6c* on chloride uptake ($J_{in}^{Cl^-}$) in 5–7 d.p.f. zebrafish larvae reared in control water or in water containing high [$NaHCO_3$] (2 or 5 mmol l^{-1}). Differences between morpholino- and sham-injected fish are indicted by daggers (P<0.05). Differences within either the sham- or morpholino-injected fish as a function of ambient [$NaHCO_3$] are indicated by dissimilar letters (lower case for shams; upper case for morphants).

Cl^-/HCO_3^- exchangers in the zebrafish gill also are localized to base-secreting MR cells, a proposition that will require further testing.

Do SLC26A3, A4 and A6c all play a role in Cl^- uptake in zebrafish larvae?

Under control conditions, Cl^- uptake was significantly reduced only in those fish experiencing knockdown of *zA3*, a result which suggests that zA3-mediated Cl^-/HCO_3^- exchange may be the most significant route of Cl^- entry when considering the three SLC26 paralogs investigated in this study. Additionally, we suggest that zA6c is playing a role; whereas Cl^- uptake was not statistically reduced after *za6c* knockdown, there was an obvious downward trend (P=0.084; Fig. 7) and similar to *za3* knockdown, base efflux was significantly decreased in the *zA6c* morphants (Fig. 11). Given the likelihood of multiple routes of Cl^- uptake, the results of single knockdown experiments should be interpreted cautiously. Thus, while knockdown of *za4* did not decrease Cl^- uptake under control conditions, this may simply reflect compensatory increases in Cl^- uptake *via* other routes including zA3- and zA6c-mediated Cl^-/HCO_3^- exchange. Finally, because other isoforms of zA6 exist (see Fig. 1), further studies will be required to fully elucidate the relative roles of the various zA6 genes.

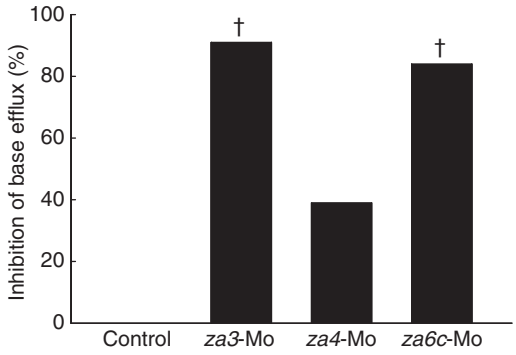

Fig. 11. The inhibitory effects of morpholino antisense oligonucleotides (MO) knockdown of SLC26 genes on base excretion in 5–7 d.p.f. zebrafish larvae. Significant differences (determined from absolute flux data) from control (sham-injected) larvae are denoted by daggers (one-way ANOVA; P<0.05).

The effects of SLC26 gene knockdown on Cl^- uptake were more pronounced (especially for *za4* and *za6c*) in fish previously exposed to either low environmental [Cl^-] or elevated ambient [HCO_3^-]. These findings, together with the observation of increased levels of SLC26 mRNA, suggest that the increased rates of Cl^- uptake associated with these treatments (see also Boisen et al., 2003) probably arise, in part, from transcriptionally mediated increases in zA3, zA4 and zA6c expression. Thus, Cl^- uptake, although unresponsive to *za4* knockdown under control conditions, was markedly reduced by this treatment in fish raised in water containing low Cl^- or 5 mm $NaHCO_3$ (Figs 7 and 10). Interestingly, SLC26 gene knockdown was completely without effect on Cl^- uptake in fish raised in water with a high [Cl^-] (but assayed in control water). These finding suggest that expression of the SLC26 exchangers (zA3, zA4 and zA6c) was decreased in these fish (note that mRNA levels, however, were unaffected) and that Cl^- uptake may have been occurring *via* other routes.

A comparison of the fish gill and mammalian kidney

Similar to the fish gill, which absorbs Cl^- from water, the mammalian kidney reabsorbs Cl from tubular urine using a variety of transport proteins including members of the SLC4 and SLC26 gene families (Romero et al., 2004; Mount and Romero, 2004; Alper, 2006; Pushkin and Kurtz, 2006; Soleimani and Xu, 2006; Sindic et al., 2007). The SLC26 genes that have been implicated are A4 (localized to the apical membrane of β-intercalated cells) and A6 (localized to apical membrane of proximal tubule cells). Additionally, SLC26A6 together with basolateral SLC26A1 play integral roles in oxalate, formate and sulfate reabsorption at the proximal tubule. Similarly, SLC26A1 has been implicated in renal sulfate transport in eel (*Anguilla japonica*) (Nakada et al., 2005) and rainbow trout (Katoh et al., 2006). Little is known about the role of SLC4

Cl^-/HCO_3^- exchangers in the fish kidney although SLC4A2 (AE2) has been identified in the kidney of larval zebrafish (Shmukler et al., 2005; Shmukler et al., 2008). Interestingly, SLC26A3, shown in this study as a route of Cl^- absorption in zebrafish larvae, is not expressed in the mammalian kidney. Another major difference between the kidney and gill models is that the fish gill can absorb Cl^- from very dilute water where there is no obvious favorable chemical gradient for Cl^- to allow electroneutral Cl^-/HCO_3^- exchange. Two possible scenarios may account for the ability of FW fish to absorb Cl^- from dilute media. First, the intracellular levels of HCO_3^-, although too low at the macroscopic level to fuel Cl^-/HCO_3^- exchange, might be enriched within micro-domains near the apical membrane by the integrated actions of carbonic anhydrase and V-type H^+-ATPase (Tresguerres et al., 2006). Second, one or more of the anion transporters may be operating in an electrogenic mode. For example, the SCL26A6 teleost fish paralogs that have been characterized to date appear to be electrogenic operating in an $nHCO_3^-/Cl^-$ mode (Grosell et al., 2009; Kurita et al., 2008). This transport stoichiometry would be favorable for Cl^-/HCO_3^- exchange across the apical membrane because the inside negative membrane potential would fuel the activity of $nHCO_3^-/Cl^-$ exchange by SLC26A6.

Zebrafish exhibit an unusually high affinity for Cl^- uptake (K_m 8 μmol l^{-1}) when acclimated to soft water (43 μmol l^{-1} Cl^-) (Boisen et al., 2003). This raises the obvious question as to how the SLC26 exchangers might be involved in branchial Cl^- uptake given that they normally exhibit K_m values for Cl^-/HCO_3^- exchange in the low millimolar range (e.g. Shcheynikov et al., 2006). The simplest explanation (also see Grosell et al., 2009) is that one or more of the zebrafish SLC26 Cl^- transporters exhibit unusually low K_m values in comparison to orthologous mammalian genes. Clearly this is an area that warrants further research.

This work was financially supported by NSERC Discovery and RTI grants to S.F.P. and M.E.E. and a NSF grant (IOB 0743903) to M.G. We are grateful to Vishal Saxena for excellent technical assistance.

REFERENCES

Alper, S. L. (2006). Molecular physiology of SLC4 anion exchangers. *Exp. Physiol.* **91**, 153-161.

Alper, S. L., Darman, R. B., Chernova, M. N. and Dahl, N. K. (2002). The AE gene family of Cl^-/HCO_3^- exchangers. *J. Nephrol.* **15 Suppl. 5**, S41-S53.

Bielmyer, G. K., Grosell, M., Paquin, P. R., Mathews, R., Wu, K. B., Santore, R. C. and Brix, K. V. (2007). Validation study of the acute biotic ligand model for silver. *Environ. Toxicol. Chem.* **26**, 2241-2246.

Boisen, A. M., Amstrup, J., Novak, I. and Grosell, M. (2003). Sodium and chloride transport in soft water and hard water acclimated zebrafish (*Danio rerio*). *Biochim. Biophys. Acta* **1618**, 207-218.

Braun, M., Steele, S. L., Ekker, M. and Perry, S. F. (2009). Nitrogen excretion in developing zebrafish (*Danio rerio*): a role for Rh proteins and urea transporters. *Am. J. Physiol.* **296**, F994-F1005.

Cameron, B. A., Perry, S. F., Wu, C. B., Ko, K. and Tufts, B. L. (1996). Bicarbonate permeability and immunological evidence for an anion exchanger-like protein in the red blood cells of the sea lamprey, *Petromyzon marinus*. *J. Comp. Physiol. B* **166**, 197-204.

Chang, I. C. and Hwang, P. P. (2004). Cl^- uptake mechanism in freshwater-adapted tilapia (*Oreochromis mossambicus*). *Physiol. Biochem. Zool.* **77**, 406-414.

Chang, I. C., Lee, T. H., Yang, C. H., Wei, Y. Y., Chou, F. I. and Hwang, P. P. (2001). Morphology and function of gill mitochondria-rich cells in fish acclimated to different environments. *Physiol. Biochem. Zool.* **74**, 111-119.

Chang, I. C., Wei, Y. Y., Chou, F. I. and Hwang, P. P. (2003). Stimulation of Cl^- uptake and morphological changes in gill mitochondria-rich cells in freshwater tilapia (*Oreochromis mossambicus*). *Physiol. Biochem. Zool.* **76**, 544-552.

Chang, W. J., Horng, J. L., Yan, J. J., Hsiao, C. D. and Hwang, P. P. (2009). The transcription factor, glial cell missing 2, is involved in differentiation and functional regulation of H^+-ATPase-rich cells in zebrafish (*Danio rerio*). *Am. J. Physiol.* **296**, R1192-R1201.

Claiborne, J. B. (1998). Acid-base regulation. In *The Physiology of Fishes*, vol. 2 (ed. David Evans), pp. 171-198. Boca Raton, FL: CRC Press.

De Renzis, G. (1975). The branchial chloride pump in the goldfish *Carassius auratus*: relationship between Cl^-/HCO_3^- and Cl^-/Cl^- exchanges and the effect of thiocyanate. *J. Exp. Biol.* **63**, 587-602.

De Renzis, G. and Maetz, J. (1973). Studies on the mechanism of chloride absorption by the goldfish gill: relation with acid-base regulation. *J. Exp. Biol.* **59**, 339-358.

Eisen, J. S. and Smith, J. C. (2008). Controlling morpholino experiments: don't stop making antisense. *Development* **135**, 1735-1743.

Epstein, F. H., Maetz, J. and De Renzis, G. (1973). Active transport of chloride by the teleost gill: inhibition by thiocyanate. *Am. J. Physiol.* **224**, 1295-1299.

Evans, D. H. (2008). Teleost fish osmoregulation: what have we learned since August Krogh, Homer Smith, and Ancel Keys. *Am. J. Physiol.* **295**, R704-R713.

Evans, D. H., Piermarini, P. M. and Potts, W. T. W. (1999). Ionic transport in the fish gill epithelium. *J. Exp. Zool.* **283**, 641-652.

Evans, D. H., Piermarini, P. M. and Choe, K. P. (2005). The multifunctional fish gill: dominant site of gas exchange, osmoregulation, acid-base regulation, and excretion of nitrogenous waste. *Physiol. Rev.* **85**, 97-177.

Goss, G. G. and Perry, S. F. (1993). Physiological and morphological regulation of acid-base status during hypercapnia in rainbow trout (*Oncorhynchus mykiss*). *Can. J. Zool.* **71**, 1673-1680.

Goss, G. G. and Perry, S. F. (1994). Different mechanisms of acid-base regulation in rainbow trout (*Oncorhynchus mykiss*) and American eel (*Anguilla rostrata*) during $NaHCO_3$ infusion. *Physiol. Zool.* **67**, 381-406.

Goss, G. G., Laurent, P. and Perry, S. F. (1992). Evidence for a morphological component in the regulation of acid-base balance in hypercapnic catfish (*Ictalurus nebulosus*). *Cell. Tissue Res.* **268**, 539-552.

Goss, G. G., Laurent, P. and Perry, S. F. (1994). Gill morphology during hypercapnia in brown bullhead (*I. nebulosus*): role of chloride cells and pavement cells in acid-base regulation. *J. Fish Biol.* **45**, 705-718.

Goss, G. G., Adamia, S. and Galvez, F. (2001). Peanut lectin binds to a subpopulation of mitochondria-rich cells in the rainbow trout gill epithelium. *Am. J. Physiol.* **281**, R1718-R1725.

Grosell, M., Mager, E. M., Williams, C. and Taylor, J. R. (2009). High rates of HCO_3^- secretion and Cl^- absorption against adverse gradients in the marine teleost intestine: the involvement of an electrogenic anion exchanger and H^+-pump metabolon? *J. Exp. Biol.* **212**, 1684-1696.

Hiroi, J., McCormick, S. D., Ohtani-Kaneko, R. and Kaneko, T. (2005). Functional classification of mitochondrion-rich cells in euryhaline Mozambique tilapia (*Oreochromis mossambicus*) embryos, by means of triple immunofluorescence staining for Na^+/K^+-ATPase, $Na^+/K^+/2Cl^-$ cotransporter and CFTR anion channel. *J. Exp. Biol.* **208**, 2023-2036.

Horng, J. L., Lin, L. Y., Huang, C. J., Katoh, F., Kaneko, T. and Hwang, P. P. (2007). Knockdown of V-ATPase subunit A (atp6v1a) impairs acid secretion and ion balance in zebrafish (*Danio rerio*). *Am. J. Physiol.* **292**, R2068-R2076.

Hwang, P. P. and Lee, T. H. (2007). New insights into fish ion regulation and mitochondrion-rich cells. *Comp. Biochem. Physiol.* **48**, 479-497.

Katoh, F., Tresguerres, M., Lee, K. M., Kaneko, T., Aida, K. and Goss, G. G. (2006). Cloning of rainbow trout SLC26A1: involvement in renal sulfate secretion. *Am. J. Physiol.* **290**, R1468-R1478.

Krogh, A. (1937). Osmotic regulation in freshwater fishes by active absorption of chloride ions. *Z. Vgl. Physiol.* **24**, 656-666.

Krogh, A. (1938). The active absorption of ions in some freshwater animals. *Z. Vgl. Physiol.* **25**, 335-350.

Kudrycki, K. E. and Shull, G. E. (1989). Primary structure of the rat kidney band 3 anion exchange protein deduced from a cDNA. *J. Biol. Chem.* **264**, 8185-8192.

Kurita, Y., Nakada, T., Kato, A., Doi, H., Mistry, A. C., Chang, M. H., Romero, M. F. and Hirose, S. (2008). Identification of intestinal bicarbonate transporters involved in formation of carbonate precipitates to stimulate water absorption in marine teleost fish. *Am. J. Physiol.* **294**, R1402-R1412.

Laurent, P., Chevalier, C. and Wood, C. M. (2006). Appearance of cuboidal cells in relation to salinity in gills of *Fundulus heteroclitus*, a species exhibiting branchial Na^+ but not Cl^- uptake in freshwater. *Cell Tissue Res.* **325**, 481-492.

Lin, L. Y., Horng, J. L., Kunkel, J. G. and Hwang, P. P. (2005). Proton pump-rich cell secretes acid in skin of zebrafish larvae. *Am. J. Physiol.* **290**, C371-C378.

Lin, T. Y., Liao, B. K., Horng, J. L., Yan, J. J., Hsiao, C. D. and Hwang, P. P. (2008). Carbonic anhydrase 2-like a and 15a are involved in acid-base regulation and Na^+ uptake in zebrafish H^+-ATPase-rich cells. *Am. J. Physiol.* **294**, C1250-C1260.

Maetz, J. and Garcia Romeu, F. (1964). The mechanism of sodium and chloride uptake by the gills of a freshwater fish, *Carassius auratus*: II. Evidence for $NH4^+/Na^+$ and HCO_3^-/Cl^- exchanges. *J. Gen. Physiol.* **47**, 1209-1227.

Marshall, W. S. (1995). Transport processes in isolated teleost epithelia: opercular epithelium and urinary bladder. In *Cellular and Molecular Approaches to Fish Ionic Regulation* (ed. C. M. Wood and T. J. Shuttleworth), pp. 1-23. New York: Academic Press.

Marshall, W. S. (2002). Na^+, Cl^-, Ca^{2+} and Zn^{2+} transport by fish gills: retrospective review and prospective synthesis. *J. Exp. Zool.* **293**, 264-283.

Marshall, W. S. and Grosell, M. (2006). Ion transport, osmoregulation and acid-base balance. In *The Physiology of Fishes* (ed. D. H. Evans and J. B. Claiborne), pp. 177-230. Boca Raton, FL: CRC Press.

McDonald, D. G. and Wood, C. M. (1981). Branchial and renal acid and ion fluxes in the rainbow trout, *Salmo gairdneri*, at low environmental pH. *J. Exp. Biol.* **93**, 101-118.

Morgan, I. J. and Potts, W. T. W. (1995). The effects of thiocyanate on the intracellular ion concentrations in branchial epithelial cells of brown trout. *J. Exp. Biol.* **198**, 1229-1232.

Morgan, I. J., Potts, W. T. W. and Oates, K. (1994). Intracellular ion concentrations in branchial epithelial cells of brown trout (*Salmo trutta* l) determined by x-ray microanalysis. *J. Exp. Biol.* **194**, 139-151.

Mount, D. B. and Romero, M. F. (2004). The SLC26 gene family of multifunctional anion exchangers. *Pflugers Arch.* **447**, 710-721.

Nakada, T., Zandi-Nejad, K., Kurita, Y., Kudo, H., Broumand, V., Kwon, C. Y., Mercado, A., Mount, D. B. and Hirose, S. (2005). Roles of Slc13a1 and Slc26a1 sulfate transporters of eel kidney in sulfate homeostasis and osmoregulation in freshwater. *Am. J. Physiol.* **289**, R575-R585.

Nasevicius, A. and Ekker, S. C. (2000). Effective targeted gene 'knockdown' in zebrafish. *Nat. Genet.* **26**, 216-220.
Ohana, E., Yang, D., Shcheynikov, N. and Muallem, S. (2009). Diverse transport modes by the Solute Carrier 26 family of anion transporters. *J. Physiol.* **587**, 2179-2185.
Pan, T. C., Liao, B. K., Huang, C. J., Lin, L. Y. and Hwang, P. P. (2005). Epithelial Ca^{2+} channel expression and Ca^{2+} uptake in developing zebrafish. *Am. J. Physiol.* **289**, R1202-R1211.
Patrick, M. L., Part, P., Marshall, W. S. and Wood, C. M. (1997). Characterization of ion and acid-base transport in the fresh water adapted mummichog (*Fundulus heteroclitus*). *J. Exp. Zool.* **279**, 208-219.
Perry, S. F. and Gilmour, K. M. (2006). Acid-base balance and CO_2 excretion in fish: unanswered questions and emerging models. *Respir. Physiol. Neurobiol.* **154**, 199-215.
Perry, S. F. and Goss, G. G. (1994). The effects of experimentally altered gill chloride cell surface area on acid-base regulation in rainbow trout during metabolic alkalosis. *J. Comp. Physiol. A* **164**, 327-336.
Perry, S. F. and Randall, D. J. (1981). Effects of amiloride and SITS on branchial ion fluxes in rainbow trout, *Salmo gairdneri*. *J. Exp. Zool.* **215**, 225-228.
Perry, S. F., Haswell, M. S., Randall, D. J. and Farrell, A. P. (1981). Branchial ionic uptake and acid-base regulation in the rainbow trout, *Salmo gairdneri*. *J. Exp. Biol.* **92**, 289-303.
Perry, S. F., Furimsky, M., Bayaa, M., Georgalis, T., Nickerson, J. G. and Moon, T. W. (2003a). Integrated involvement of Na^+/HCO_3^- cotransporters and V-type H^+-ATPases in branchial and renal acid-base regulation in freshwater fishes. *Biochem. Biophys. Acta* **1618**, 175-184.
Perry, S. F., Shahsavarani, A., Georgalis, T., Bayaa, M., Furimsky, M. and Thomas, S. L. Y. (2003b). Channels, pumps and exchangers in the gill and kidney of freshwater fishes: Their role in ionic and acid-base regulation. *J. Exp. Zool.* **300**, 53-62.
Pfaffl, M. W. (2001). A new mathematical model for relative quantification in real-time RT-PCR. *Nucleic Acids Res.* **29**, 2002-2007.
Piermarini, P. M., Verlander-Reed, J. V., Royaux, I. E. and Evans, D. H. (2001). Immunochemical evidence for pendrin in the gills of the euryhaline Atlantic stingray (*Dasyatis sabina*): implications for ionic and acid/base regulation. *Am. Zool.* **41**, 1556.
Piermarini, P. M., Verlander, J. W., Royaux, I. E. and Evans, D. H. (2002). Pendrin immunoreactivity in the gill epithelium of a euryhaline elasmobranch. *Am. J. Physiol.* **283**, R983-R992.
Pisam, M., Caroff, A. and Rambourg, A. (1987). Two types of chloride cells in the gill epithelium of a freshwater adapted euryhaline fish: *Lebistes reticulatus*; their modification during adaptation to seawater. *Am. J. Anat.* **179**, 40-50.
Preest, M. R., Gonzalez, R. J. and Wilson, R. W. (2005). A pharmacological examination of Na^+ and Cl^- transport in two species of freshwater fish. *Physiol. Biochem. Zool.* **78**, 259-272.
Pushkin, A. and Kurtz, I. (2006). SLC4 base (HCO_3^-, CO_3^{2-}) transporters: classification, function, structure, genetic diseases, and knockout models. *Am. J. Physiol.* **290**, F580-F599.
Rombough, P. (2002). Gills are needed for ionoregulation before they are needed for O_2 uptake in developing zebrafish, *Danio rerio*. *J. Exp. Biol.* **205**, 1787-1794.
Rombough, P. (2007). The functional ontogeny of the teleost gill: which comes first, gas or ion exchange? *Comp. Biochem. Physiol.* **148A**, 732-742.
Romero, M. F., Fulton, C. M. and Boron, W. F. (2004). The SLC4 family of HCO_3^- transporters. *Pflugers Arch.* **447**, 495-509.
Romero, M. F., Chang, M. H., Plata, C., Zandi-Nejad, K., Mercado, A., Broumand, V., Sussman, C. R. and Mount, D. B. (2006). Physiology of electrogenic SLC26 paralogues. *Novartis Found. Symp.* **273**, 126-138.
Shaner, N. C., Campbell, R. E., Steinbach, P. A., Giepmans, B. N., Palmer, A. E. and Tsien, R. Y. (2004). Improved monomeric red, orange and yellow fluorescent proteins derived from *Discosoma* sp. red fluorescent protein. *Nat. Biotechnol.* **22**, 1567-1572.
Shcheynikov, N., Wang, Y., Park, M., Ko, S. B., Dorwart, M., Naruse, S., Thomas, P. J. and Muallem, S. (2006). Coupling modes and stoichiometry of Cl^-/HCO_3^- exchange by slc26a3 slc26a6. *J. Gen. Physiol.* **127**, 511-524.
Shih, T. H., Horng, J. L., Hwang, P. P. and Lin, L. Y. (2008). Ammonia excretion by the skin of zebrafish (*Danio rerio*) larvae. *Am. J. Physiol.* **295**, C1625-C1632.
Shmukler, B. E., Kurschat, C. E., Ackermann, G. E., Jiang, L., Zhou, Y., Barut, B., Stuart-Tilley, A. K., Zhao, J., Zon, L. I., Drummond, I. A. et al. (2005). Zebrafish slc4a2/ae2 anion exchanger: cDNA cloning, mapping, functional characterization, and localization. *Am. J. Physiol.* **289**, F835-F849.
Shmukler, B. E., Clark, J. S., Hsu, A., Vandorpe, D. H., Stewart, A. K., Kurschat, C. E., Choe, S. K., Zhou, Y., Amigo, J., Paw, B. H. et al. (2008). Zebrafish ae2.2 encodes a second slc4a2 anion exchanger. *Am. J. Physiol.* **294**, R1081-R1091.
Sindic, A., Chang, M. H., Mount, D. B. and Romero, M. F. (2007). Renal physiology of SLC26 anion exchangers. *Curr. Opin. Nephrol. Hypertens.* **16**, 484-490.
Soleimani, M. and Xu, J. (2006). SLC26 chloride/base exchangers in the kidney in health and disease. *Semin. Nephrol.* **26**, 375-385.
Soleimani, M., Greeley, T., Petrovic, S., Wang, Z., Amlal, H., Kopp, P. and Burnham, C. E. (2001). Pendrin: an apical $Cl^-/OH^-/HCO_3^-$ exchanger in the kidney cortex. *Am. J. Physiol.* **280**, F356-F364.
Sullivan, G. V., Fryer, J. N. and Perry, S. F. (1996). Localization of mRNA for proton pump (H^+-ATPase) and Cl^-/HCO_3^- exchanger in rainbow trout gill. *Can. J. Zool.* **74**, 2095-2103.
Tomasso, J. R., Jr and Grosell, M. (2005). Physiological basis for large differences in resistance to nitrite among freshwater and freshwater-acclimated euryhaline fishes. *Environ. Sci. Technol.* **39**, 98-102.
Tresguerres, M., Katoh, F., Orr, E., Parks, S. K. and Goss, G. G. (2006). Chloride uptake and base secretion in freshwater fish: a transepithelial ion-transport metabolon? *Physiol. Biochem. Zool.* **79**, 981-996.
Trevarrow, B., Marks, D. L. and Kimmel, C. B. (1990). Organization of hindbrain segments in the zebrafish embryo. *Neuron* **4**, 669-679.
Tseng, D. Y., Chou, M. Y., Tseng, Y. C., Hsiao, C. D., Huang, C. J., Kaneko, T. and Hwang, P. P. (2009). Effects of stanniocalcin 1 on calcium uptake in zebrafish (*Danio rerio*) embryo. *Am. J. Physiol.* **296**, R549-R557.
Varsamos, S., Nebel, C. and Charmantier, G. (2005). Ontogeny of osmoregulation in postembryonic fish: a review. *Comp. Biochem. Physiol.* **141A**, 401-429.
Verdouw, H., van Echteld, C. J. A. and Dekkers, E. M. J. (1978). Ammonia determinations based on indophenol formation with sodium salicylate. *Water Res.* **12**, 399-402.
Westerfield, M. (2007). *The Zebrafish Book*, 5th edn. Eugene, OR: University of Oregon Press.
Wilson, J. M., Laurent, P., Tufts, B. L., Benos, D. J., Donowitz, M., Vogl, A. W. and Randall, D. J. (2000). NaCl uptake by the branchial epithelium in freshwater teleost fish: an immunological approach to ion-transport protein localization. *J. Exp. Biol.* **203**, 2279-2296.
Yan, J. J., Chou, M. Y., Kaneko, T. and Hwang, P. P. (2007). Gene expression of Na^+/H^+ exchanger in zebrafish H^+-ATPase-rich cells during acclimation to low-Na^+ and acidic environments. *Am. J. Physiol.* **293**, C1814-C1823.